

1
2
3
4
5

AN INTEGRATIVE ANALYSIS OF CANCER GENE EXPRESSION STUDIES USING BAYESIAN LATENT FACTOR MODELING

6
7
8

BY DANIEL MERL^{*}, JULIA LING-YU CHEN^{†,‡}, JEN-TSAN
CHI^{†,‡}, AND MIKE WEST^{*,‡}

9
10

Duke University, Durham NC, USA

11
12
13
14
15
16
17
18
19
20
21
22
23
24
25
26
27
28

We present an applied study in cancer genomics for integrating data and inferences from laboratory experiments on cancer cell lines with observational data obtained from human breast cancer studies. The biological focus is on improving understanding of transcriptional responses of tumors to changes in the pH level of the cellular microenvironment. The statistical focus is on connecting experimentally defined biomarkers of such responses to clinical outcome in observational studies of breast cancer patients. Our analysis exemplifies a general strategy for accomplishing this kind of integration across contexts. The statistical methodologies employed here draw heavily on Bayesian sparse factor models for identifying, modularizing, and correlating with clinical outcome these *signatures* of aggregate changes in gene expression. By projecting patterns of biological response linked to specific experimental interventions into observational studies where such responses may be evidenced via variation in gene expression across samples, we are able to define biomarkers of clinically relevant physiological states and outcomes that are rooted in the biology of the original experiment. Through this approach we identify microenvironment-related prognostic factors capable of predicting long term survival in two independent breast cancer datasets. These results suggest possible directions for future laboratory studies, as well as indicate the potential for therapeutic advances through targeted disruption of specific pathway components.

29
30
31
32
33
34
35

1. Introduction. Cancer progression involves a complex interaction of genetic and genomic factors that jointly subvert normal cell development. The genomic component, which encompasses gene expression and regulation, is substantially impacted by the biochemical composition of the local environment in which a cell grows. So-called *micro-environmental* parameters,

36

^{*}Department of Statistical Science

37

[†]Department of Molecular Genetics & Microbiology

38

[‡]Institute for Genome Sciences and Policy

39
40
41

Keywords and phrases: Acidosis and neutralization pathways in cancer, Bayesian latent factor models, Breast cancer genomics, Gene expression signatures, Integrative cancer genomics, Micro-environmental parameters in cancer, Weibull survival models

1 including levels of oxidation, lactate, acidity, nutrients of various kinds, and 1
2 other factors affecting physical interactions between cells, are increasingly 2
3 studied for their potential to improve our understanding of cancer biology, 3
4 and for their promise to lead to new therapeutic strategies. Changes in such 4
5 parameters can impact gene transcription, which in turn impacts protein 5
6 production. Variation in these fundamental parameters can therefore induce 6
7 a cascade of effects, producing disruptions of normal cellular processes in 7
8 downstream biological pathways (9). For example, changes to the pH level 8
9 in the cellular environment may effect glycolysis, thus impacting on numer- 9
10 ous genes involved in the glycolysis pathway. Some of these genes may also 10
11 play roles in the regulation of cell growth, and their suppression may engen- 11
12 der tumorigenesis and promote the aggressive advance of existing cancerous 12
13 states. Microarray gene expression assays can be used to generate data on 13
14 the transcriptional response of cancer cells to controlled manipulations of en- 14
15 vironmental factors such as pH. This data is useful for characterizing these 15
16 *micro-environmental response pathways*. 16

17 Our study concerns changes to cellular pH levels, and the resulting *neu-* 17
18 *tralization* and *lactic acidosis response pathways*. Section 2 describes the ap- 18
19 plication of sparse Bayesian regression models (15; 21) to microarray data 19
20 generated through a series of laboratory experiments on cultured breast 20
21 tumor cells in which cellular pH levels were manipulated in a controlled 21
22 manner. These analyses yield statistical *expression signatures* of the cellu- 22
23 lar responses to various interventions on the pH level. The main challenge 23
24 lies in relating these signatures, and the biological pathways they charac- 24
25 terize, to variation in gene expression across large samples of human breast 25
26 tumors. This integration of *in-vitro* and *in-vivo* data sets is the driving fo- 26
27 cus of this and related studies. In addition to comprising a detailed study 27
28 of new data and experimental results, through which are generated several 28
29 directions for biomedical research, this work exemplifies an overall strategy 29
30 for cross-study, integrative analysis of gene expression data for exploring 30
31 and relating pathway-related experimental findings to clinical contexts and 31
32 patient outcomes. 32

33 When considering variability in expression patterns of genes in obser- 33
34 vational tumor data, we face questions of differences due to the differing 34
35 contexts. It is to be expected that a tumor *in-vivo* evidences far more com- 35
36 plex and heterogeneous biological variation than in the controlled *in-vitro* 36
37 setting, and this will be manifest in measures of gene expression. Normal cell 37
38 processes held in quiescence in cell cultures may when active co-regulate the 38
39 expression of relevant signature genes in *in-vivo*, confounding the pattern of 39
40 expression that was evident *in-vitro*. Hence, when aiming to translate exper- 40
41

1 imental findings to tumor populations, thereby providing a mapping of an 1
 2 *in vitro* signature to its *in-vivo* counterpart, we require statistical models ca- 2
 3 pable of discovering and representing the additional complexity surrounding 3
 4 and interacting with the original response signature. Section 3 describes our 4
 5 analysis of a large and heterogeneous breast cancer data set using sparse 5
 6 latent factor models (26; 21; 2) that satisfy these desiderata. This analy- 6
 7 sis includes a targeted factor search that facilitates estimation of statistical 7
 8 factors associated with an initial set of genes underlying the *in-vitro* exper- 8
 9 imental signatures. The factors discovered in this way represent a modular 9
 10 decomposition of the biological patterns evident in the *in-vivo* breast cancer 10
 11 data, while retaining connections to the experimental signatures. 11

12 Section 4 discusses aspects of the biological and clinical interpretations 12
 13 of these estimated factors, which can be viewed as a refined *in-vivo* set of 13
 14 summary biomarkers of variation in the *neutralization* and *lactic acidosis* 14
 15 *response pathways* of these breast cancers. In survival analyses, we find that 15
 16 these factor model derived biomarkers have substantial prognostic value in 16
 17 connection with long-term survival, and hence the sets of genes comprising 17
 18 these factors warrant further study. We present predictive validation of this 18
 19 key finding in analyses of two separate breast cancer data sets. We then 19
 20 provide biological interpretation of one key factor that emerged from the 20
 21 evolutionary factor search, which plays a key role as a predictive variable 21
 22 in the survival analyses. It turns out that this factor is a single compo- 22
 23 nent of a specific biological pathway that has previously been noted as a 23
 24 risk biomarker in cancer, but not, to date, connected at all into response 24
 25 pathways linked with variation in cellular pH. This finding has generated 25
 26 follow-on biological research and initiated a new line of experimentation on 26
 27 the role of this pathway in connection with cancer cell micro-environmental 27
 28 influences. 28

29 2. Neutralization Experiments and Analysis. 29

30 31
 32 2.1. *Biological and Experimental Context.* Investigating the effects of 31
 33 changes in the micro-environment in which cells grow is of increasing interest 32
 34 in cancer research. The tumor micro-environment is typically characterized 33
 35 by oxygen depletion, high lactate and extracellular acidosis coupled with 34
 36 vascular leakage, glucose and energy deprivation. These and other micro- 35
 37 environmental features vary widely across tumors and generally exhibit sub- 36
 38 stantial temporal and spatial differences in a tumor. Micro-environmental 37
 39 stresses trigger biochemical changes in cancer cells that directly modulate 38
 40 physiological, metabolic and ultimately clinical phenotypes. Improved un- 39
 41 derstanding of the molecular mechanisms of such tumor responses holds 40
 41

TABLE 1
Summary of neutralization/acidosis experiments. Cell entries indicate the number of replicates per experimental group.

growth condition	exposure condition				
	pH 7.4		pH 6.7		pH 5.5
	1hr	4hr	1hr	4hr	4hr
pH 7.4	3x	3x	3x	3x	3x
pH 6.7	3x	3x	3x	3x	

promise for immediate translational impact and clinical care, as relevant therapies can be brought to bear to modify the micro-environment.

Currently, with the exception of hypoxia, very little is understood about how each individual stress affects cellular phenotypes and tumor progression. To examine how cancer cells respond to increased acidity or pH neutralization at different time points, MCF7 cell cultures (a commonly-used breast tumor cell line) were grown in neutral media and then exposed to varying interventions in several assays in parallel. For some cells, lactic acid was added to the medium (25 mM lactic acid at pH 6.7) for 1 and 4 hours; others cells experienced strong lactic acidosis conditions (25 nM lactic acid at pH 5.5) for 4 hours. Similarly, the effects of neutralization were assayed by shifting the MCF7 cultures from overnight lactic acidosis conditions at pH 6.7 to neutral regular media at pH 7.4 for 1 and 4 hours. Control cells were grown in each starting condition (neutral conditions and lactic acidosis conditions). The complete set of experiments is summarized in Table 1. The mRNA extracted from each of the resulting $n = 27$ batches of MCF7 cultures was purified using Ambion miRVana RNA purification kits and standard microarray assays were performed using Affymetrix U133 Plus 2 Genechip platforms. All raw microarray data were preprocessed using RMA (13), the log (base 2) scale output of which were used in all ensuing statistical analyses.

2.2. Cellular Response Signatures. Quantitative summaries of the cellular responses to lactic acidosis and neutralization treatments were obtained using a standard sparse multivariate regression model (15; 21). We analyzed 19,375 genes (technically, probe-sets from the Affymetrix array; we will use “gene” and “probe” interchangeably) whose median expression level is at least 5.5 and whose expression ranges more than 0.5-fold across the $n = 27$ experimental samples. Let X^{exp} denote the $19,375 \times 27$ matrix of expression values. Rows represent genes and columns correspond to three replicate samples for each of the following experimental groups: (i) control (pH 7.4 \rightarrow 7.4) at 1 hour; (ii) control at 4 hours; (iii) lactic acidosis (pH 7.4 \rightarrow 6.7) at 1

1 hour; *(iv)* lactic acidosis at 4 hours; *(v)* neutralization (pH 6.7 \rightarrow 7.4) at 1 hour; *(vi)* neutralization at 4 hours; *(vii)* acidic growth (constant pH of 6.7) at 1 hour; *(viii)* acidic growth at 4 hours; *(ix)* strong lactic acidosis (pH 7.4 \rightarrow 5.5) at 4 hours. Let H^{exp} denote the 11×27 design matrix where the first 8 rows contain binary indicators for effects associated with differential expression relative to the 1hr control group: 1hr lactic acidosis effect, 1hr neutralization effect, 1hr acidic growth effect, 4hr control effect, 4hr lactic acidosis effect (relative to 4hr control), 4hr neutralization (relative to 4hr control), 4hr acidic growth effect (relative to 4hr control), and 4hr strong lactic acidosis effect (relative to 4hr control). The last three rows contain artifact control factors derived from the first three principle components of the expression levels associated with the AFFX series control genes included on the Affymetrix microarrays. These control genes are not variably expressed in humans, and so patterns of variation across samples manifest in control genes represents systematic errors arising from different experimental conditions. Use of these artifact control factors provides opportunity for sample-specific correction of artifactual effects on genes that may otherwise result in false-discovery or obscure meaningful biological variation (following [15; 2](#)). After deriving the artifact control factors, rows corresponding to Affymetrix control genes are removed from subsequent analyses.

The model for the expression of gene g in sample i is

$$x_{g,i}^{exp} = \mu_g + \sum_{k=1}^{11} \beta_{g,k} h_{k,i}^{exp} + \nu_{g,i}$$

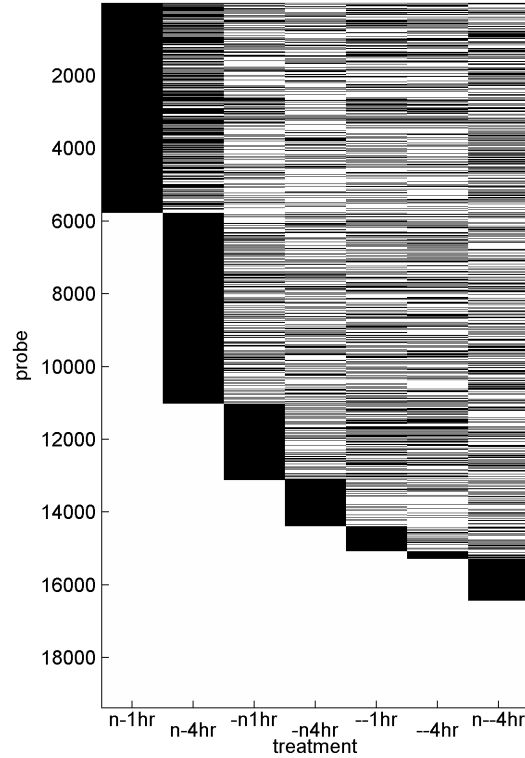
or in matrix from

$$X^{exp} = \mu 1 + BH + N$$

where μ_g denotes the mean expression of gene g in the 1hr control samples, each $\beta_{g,k}$ is the change in expression of gene g due to design factor k , and the $\nu_{g,i}$ are independent, normally distributed idiosyncratic noise terms representing residual biological variation, experimental and measurement errors with individual variances ψ_g . Sparsity is induced via prior distributions that place positive probability on $\beta_{g,k} = 0$ for each g, k pair, and resulting posterior analysis allows investigation of posterior sparsity patterns via probabilities $\pi_{g,k}^* = \Pr(\beta_{g,k} \neq 0 | X^{exp})$. Full details follow [\(15\)](#) and prior specifications, including priors for the μ_k , variance parameters and all hyper-parameters, are given in the appendix here. Posterior inference via MCMC is achieved using the BFRM software [\(24\)](#).

Figure [1](#) broadly illustrates genes uniquely associated with individual treatment effects as well as those involved in multiple responses. This gives

1 some indication of the degree of intersection of the cellular pathways being 1
 2 queried by the different treatments. Across the 8 treatments, the sparsity, 2
 3 as measured by the percent of genes for which $\pi_{g,k}^* > 0.99$, ranges from 29% 3
 4 (4 hour neutralization) to 46% (4 hour lactic acidosis). The fold-change as- 4
 5 sociated with the involved genes ($2^{|\beta_{g,k}|}$ for g such that $\pi_{g,k}^* > .99$) ranges 5
 6 from 1.06x to 13x, with a mean of 1.4x. 6
 7
 8
 9



10
11
12
13
14
15
16
17
18
19
20
21
22
23
24
25
26
27
28
29
30
31
32
33
34
35
36
37
38
39
40
41

FIG 1. Neutralization signature skeleton: black indicates genes g (rows) with posterior probability $\pi_{g,k}^* > 0.99$ for each experimental group k (columns). Genes are ordered to emphasize which genes are unique to each successive experiment relative to the previous.

The cellular response to each treatment, also called the *signature* of the treatment, is characterized by estimated effects $\beta_{g,k}^* = E(\beta_{g,k} | \beta_{g,k} \neq 0, X^{exp})$ together with the $\pi_{g,k}^*$. The ability of each signature to uniquely identify the treatment it reflects can be further explored using summary *signature scores*

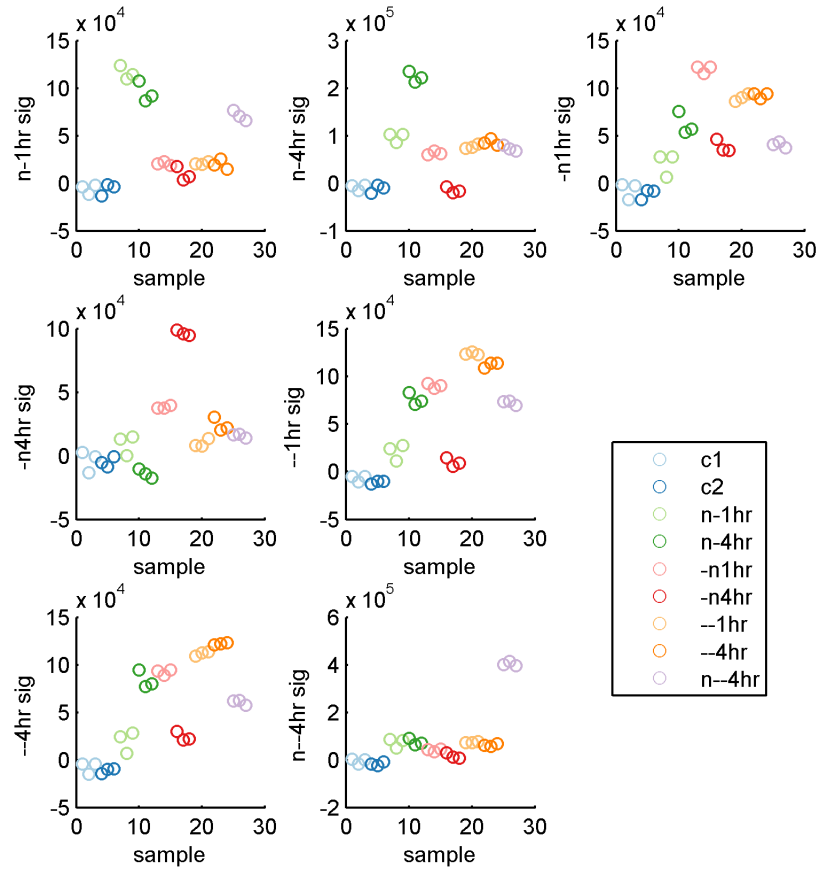


FIG 2. Neutralization treatment signature scores ($s_{k,i}$) for each sample in the original study. Separate treatment groups are color coded.

as defined in (17). Based on posterior means $\beta_{g,k}^*$ and ψ_g^* , let

$$s_{k,i} = \sum_{g=1}^{19375} \beta_{g,k}^* x_{g,i}^{exp} / \psi_g^*$$

define the score for treatment signature k on sample i . This expression is derived from the data-driven component of the Bayes factor that weighs the evidence in favor of the given signature describing the variation in a sample ($p(x_i|h_{k,i} = 1)/p(x_i|h_{k,i} = 0)$). Figure 2 shows the values of the scores associated with 7 treatment signatures plotted across samples. As expected, the highest scoring samples for each signature are those upon which that signature is based, but important connections between signatures can be identified on the basis of other high- or low-scoring treatment groups. For example, there is an inverse relationship between the 4hr acidosis score and the 4hr neutralization score. Also evident is the similarity between the 1hr and 4hr acidic growth signatures, which can also be inferred through the large intersection of the genes defining the two signatures (Figure 1).

3. Latent Factor Analysis of Breast Tumor Gene Expression.

3.1. In-Vivo Breast Cancer Data. The primary goals of this study are to uncover shared structures in the cell response signatures defined above, and to quantify the extent to which these structures can be used to predict clinical phenotypes in real human cancers. Here we make use of the gene expression data for a collection of 251 surgically removed breast tumors as reported in Miller *et. al.* (18). Affymetrix 133A and 133B GeneChip microarrays were generated for each tumor sample, and relevant clinicopathological variables were collected for each patient. This included age at diagnosis, tumor size, lymph node status (an indicator of metastatic cancer), and Elston histologic grade (a categorical rating of malignancy as deemed by pathologists). Molecular assays to identify the presence or absence of mutations in the estrogen receptor (ER), progesterone receptor (PgR), and P53 genes were also performed. These data are representative of a variety of different presentations of human breast cancer on these clinical measures.

We first evaluate the signature score as defined above for each tumor. These scores are then standardized across samples so that each vector of 27 scores for a particular signature has mean and variance equal to the mean gene-specific expression and mean gene-specific variance. This transformation places the signature scores on the same scale as gene expression in the tumor data set, thus enabling a “metagene” interpretation of a vector of scores (25; 20); see Figure 3. The relationships between the tumor signa-

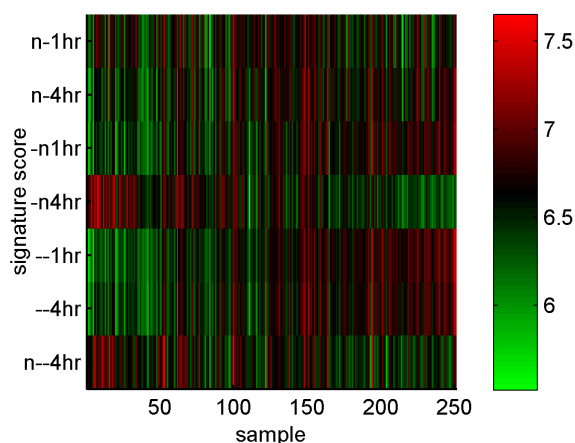


FIG 3. Initial evaluation of neutralization signature levels across tumor samples. Samples are ordered by first principle component to emphasize dominant signature gradients.

ture scores bear some similarities to those observed in the cell line study. There is once again evidence of correlation between the two acidic growth signatures and the 1hr neutralization signature. These three signatures, in turn, display patterns opposite that of the 4hr neutralization signature. The patterns are less prominent, however, than was evident in the cell culture data. Although the variation in these scores presumably relates, in part, to underlying biological variation in the activity of the lactic acidosis and neutralization response pathways within these tumors, as mentioned above the set of genes characterizing the *in-vivo* effects of lactic acidosis and neutralization may differ substantially from those characterizing the *in-vitro* responses as a result of the more complex interactions with other cellular processes.

We thus aim to refine our evaluation of the response pathway activity levels in the tumordata by using the signature scores as initial “anchors” in an analysis using sparse latent factor models. The main idea is to define statistical factors on sets of genes related to these initial scores, and to link in other genes that may connect with the different response pathways active *in-vivo*. This is accomplished as follows.

3.2. Sparse Factor Model Specification. Sparse latent factor models represent common patterns in gene expression via latent factors in which the factor-gene relationships are sparse; this notion of statistical sparsity is key for representing the intersecting subsets of genes potentially related to un-

derlying networks of biological pathways (26; 21; 16; 2). The form of the statistical model is an extension of the sparse regression model. A key part of our analysis strategy stems from augmenting the $44,592 \times 251$ matrix of gene expression data for the tumor data with the 7 values of the projected treatment signature scores. Let $p = 44,592 + 7 = 44,599$ and $n = 251$, and let X^{obs} denote the $p \times n$ matrix in which the first 7 rows are the projected scores across tumor samples, and rows $8 - p$ are the gene expression values. Here we will make use of $K = 4$ artifact control factors derived from the first four principal components of the control genes of the breast tumor microarrays. A latent factor model consisting of L latent factors is therefore:

$$x_{g,i}^{obs} = \mu_g + \sum_{k=1}^K \alpha_{g,k} \lambda_{k,i} + \sum_{l=K+1}^{K+L} \alpha_{g,l} \lambda_{l,i} + \nu_{g,i}$$

or, in matrix form,

$$X^{obs} = \mu \mathbf{1} + A\Lambda + N$$

where: (i) the first K rows of the $(K+L) \times n$ matrix Λ are the known artifact controls; (ii) the remaining L rows contain latent factor scores; (iii) the first K columns of the $p \times (K+L)$ matrix A are regression parameters on the artifact controls (changing notation from the earlier β to α for notational convenience here); (iv) the remaining L columns of A are factor loadings parameters relating factors to genes and to the projected scores; and (v) A is sparse, with sparsity pattern to be inferred along with estimation of non-zero values. The model is completed by assigning sparsity priors over columns of A , precisely as was done for B in the sparse regression model; prior specification for A , variance components and other hyper-parameters follows default recommendations for the BFRM framework (24) (see appendix).

Flexibility in representing potentially complicated patterns underlying expression is achieved using non-parametric Bayesian Dirichlet process models for the factor scores. The L -vectors $(\lambda_{K+1,i}, \dots, \lambda_{K+L,i})'$, representing the latent factor values on tumor sample i , are modelled as draws from an unknown latent factor distribution subject to a Dirichlet process prior with a multivariate normal base measure. This standard non-parametric mixture model allows great flexibility in adapting to non-normal structures commonly manifest in factor scores (2; 24).

Ensuring the identifiability of latent factors requires the use of a modified prior on A such that the leading L rows have an upper triangle of zeros and positive upper diagonal elements; i.e., for $g = 1 : L$, we have $\alpha_{g,g+K} > 0$ and $\alpha_{g,l} = 0$ for $l > g + K$. The first L variables in X^{obs} then represent “founders” of the L latent factors, with variable g associated with a $\alpha_{g,g}$ -fold change in expression due to factor g , ($g = 1, \dots, L$). It also defines an

1 hierarchical dependence on the factors, viz: 1

$$\begin{aligned}
 2 \quad x_{1,i}^{obs} &= \cdots + \alpha_{1,K+1}\lambda_{K+1,i} + \nu_{1,i} & 2 \\
 3 \quad x_{2,i}^{obs} &= \cdots + \alpha_{2,K+1}\lambda_{K+1,i} + \alpha_{2,K+2}\lambda_{K+2,i} + \nu_{2,i} & 3 \\
 4 \quad x_{3,i}^{obs} &= \cdots + \alpha_{3,K+1}\lambda_{K+1,i} + \alpha_{3,K+2}\lambda_{K+2,i} + \alpha_{3,K+3}\lambda_{K+3,i} + \nu_{3,i} & 4 \\
 5 & & 5 \\
 6 & & 6
 \end{aligned}$$

7 and so on. This structure aids the interpretation of the latent factor load- 7
 8 ings as representing interconnected components of a complex biological pro- 8
 9 cess. The latent factor scores $\lambda_{i,l}$ quantify variation across tumors for these 9
 10 expanding levels of complexity, with each additional factor accounting for 10
 11 variation in observed gene expression unaccounted for by the previous set 11
 12 of factors. With our use of projected *in-vitro* signature scores here as the 12
 13 first 7 variables, the first 7 factors will now represent patterns underlying 13
 14 co-variation in expression of sets of genes that link indirectly to these treat- 14
 15 ment signatures. Additional factors then reflect other dimensions of common 15
 16 variation in the set of genes analyzed. 16

17 **3.3. Targeted Factor Search.** Decomposition of the patterns of varia- 17
 18 tion evident in the tumor gene expression data into latent factors proceeds 18
 19 through evolutionary model search, full details of which appear in (2; 24). 19
 20 The evolutionary model search provides a computationally efficient approx- 20
 21 imation to the computationally prohibitive full factor analysis on the entire 21
 22 set of genes, and produces full posterior results for the final set of factors 22
 23 and genes. A key novelty of this approach is that we exploit the sensitivity 23
 24 of the model search procedure to its initial configuration in order explore the 24
 25 space of factor models surrounding an initial model containing 7 latent fac- 25
 26 tors and representing only the 7 response metagenes. By construction, these 26
 27 initial factors are each defined, or “founded”, by the neutralization/lactic 27
 28 acidosis treatment scores, thereby ensuring that the model search is primar- 28
 29 ily concerned with patterns of variation related to these particular response 29
 30 pathways. 30
 31

32 Evolution of this initial model proceeds as follows. Samples from the joint 32
 33 posterior distribution of model parameters are obtained through MCMC. 33
 34 Based on these fitted values, we impute inferences for all genes $g > 7$ that 34
 35 are not currently included in the model, as described in (2). Thus, after 35
 36 fitting the initial factor model which considers only the signature scores, 36
 37 we examine expression levels the full set of 44,000+ genes for evidence of 37
 38 association with the current factors. The imputation process generates ap- 38
 39 proximate probabilities $\pi_{g,l}^* = \Pr(\alpha_{g,l} \neq 0 | X^{obs})$ for all such genes g . Genes 39
 40 are ranked on the basis of these probabilities, and the model is then ex- 40
 41 panded to include a small number of the genes with largest values of the 41

1 projected $\pi_{g,l}^*$. The model is then refitted to this expanded sample, and if ap- 1
 2 propriate, the number of factors is increased in order to adapt to additional 2
 3 common patterns of expression variation now evident in the increased set 3
 4 of variables being modelled. This process is repeated until no new genes or 4
 5 factors can be added, or until the model reaches a designated maximum size. 5
 6 More details on the search strategy, including control parameters governing 6
 7 model expansion, are given in the appendix. 7

8 The initial 7-gene, 7-factor model evolved under this process to reach a 8
 9 terminal size of 500 variables (the designated maximum) incorporating 30 9
 10 latent factors. Figure 4 shows the skeleton of the factor structure, in terms 10
 11 of major patterns of gene-factor relationships. The ordering of the factors is 11
 12 determined by the model search procedure, and represents the incremental 12
 13 improvement to model fit provided by each subsequent factor. In this sense, 13
 14 each subsequent factor builds upon the complexity modeled by the previous 14
 15 factors (2). The leading 7 factors correspond to the following signatures, 15
 16 respectively: 4hr lactic acidosis, 1hr lactic acidosis, 1hr neutralization, 4hr 16
 17 strong lactic acidosis, 4hr acidic growth, 1hr acidic growth, and 4hr neutral- 17
 18 ization. Like their *in-vitro* signature counterparts, the *in-vivo* factors load- 18
 19 ings contain a great deal of sparsity. Of the 493 genes included in the final 19
 20 model, only 333 are among those identified in the *in-vitro* signature analy- 20
 21 sis. Factor 1, founded by the the 4hr lactic acidosis signature score, has 173 21
 22 genes with nonzero loadings at the 0.99 probability threshold, compared to 22
 23 8,909 in the *in-vitro* signature. 23

24 Posterior estimates of the factor loadings ($\alpha_{g,l}^* = E(\alpha_{g,l} | \alpha_{g,l} \neq 0, X^{obs})$) 24
 25 aid in generating further insights. In particular, the upper portion of the es- 25
 26 timated loadings matrix sheds light on the structure of connections between 26
 27 latent factors; see Figure 5. As described in Section 3.2, one interpretation 27
 28 of a row A is as a set of coefficients determining a linear combination of 28
 29 factor scores that predict the gene expression vector for the corresponding 29
 30 variable. The inset of Figure 5 shows that the fitted values of all 7 of signa- 30
 31 ture scores involve positive contributions from factor 1, the factor version of 31
 32 the 4hr lactic acidosis signature. Thus the pattern of 4hr lactic acidosis sig- 32
 33 nature activity across samples describes a fundamental pattern of pathway 33
 34 activation that underlies the activity patterns of the other 6 signatures. The 34
 35 seventh factor (i.e. the factor representation of the 4hr neutralization signa- 35
 36 ture) sits atop this hierarchy of pathway complexity, represented as a linear 36
 37 combination of factors 1 (4hr neutralization), 3 (1hr neutralization), 4 (4hr 37
 38 strong lactic acidosis), 5 (4hr acidic growth), plus the additional pattern of 38
 39 expression unique to this pathway. 39
 40
 41

1
2
3
4
5
6
7
8
9
10
11
12
13
14
15
16
17
18
19
20
21
22
23
24
25
26
27
28
29
30
31
32
33
34
35
36
37
38
39
40
41

1
2
3
4
5
6
7
8
9
10
11
12
13
14
15
16
17
18
19
20
21
22
23
24
25
26
27
28
29
30
31
32
33
34
35
36
37
38
39
40
41

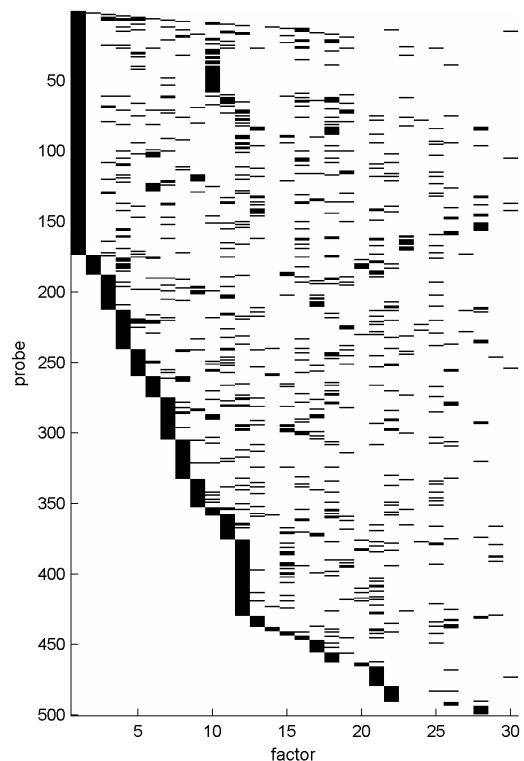


FIG 4. Skeleton of fitted factor loadings for tumor data. Black indicates variable-factor loadings with $\pi_{g,l}^* > 0.99$. The first 7 variables are the projected neutralization scores, followed by 493 genes reordered for a clear visual presentation of the sparsity structure of, and cross-talk in, gene-factor loadings.

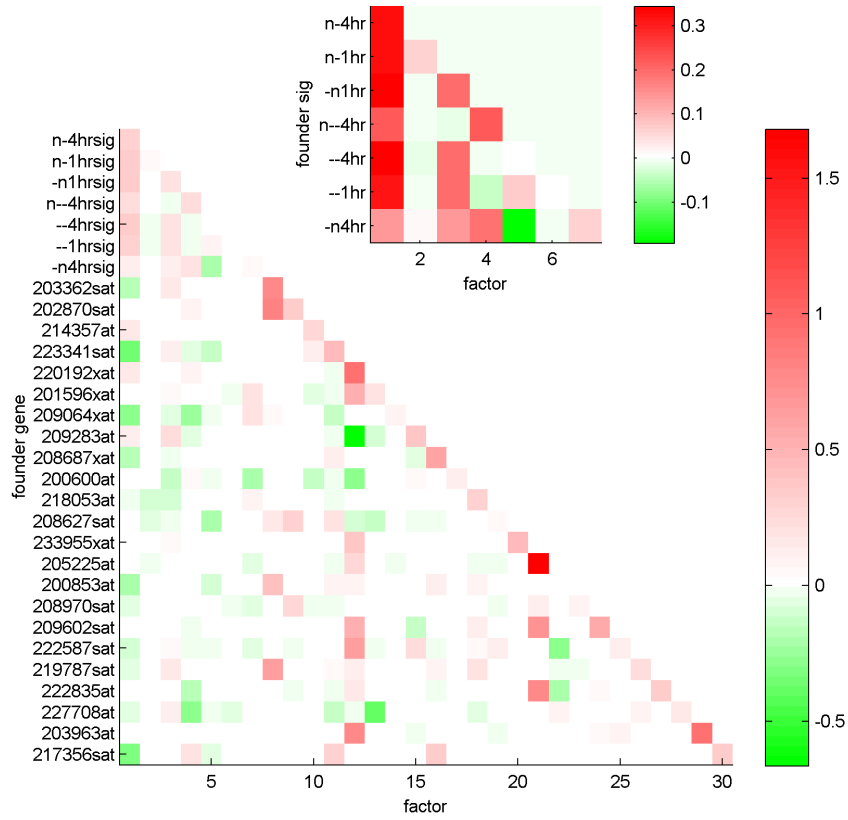


FIG 5. Heat map showing the magnitudes of the fitted factor loadings $\alpha_{g,l}^*$ for the first $L = 30$ rows of A . The founder gene for each factor is designated by its $U133+$ probe ID. The terms in each row determine a linear combination of latent factors that predict the observed expression levels of the founder gene.

4. Biomedical Connections of Factor Profiles of Neutralization Signatures.

4.1. *Factor-based Prediction of Long Term Survival.* The *in-vivo* latent factors linked to neutralization pathways represent complexity in the patterns of expression, and therefore in the levels of underlying biological pathway activation evident across the tumor samples. For this reason, latent factors can be regarded as candidate biomarkers of physiological states that link to these pathways. Our study explores this using the posterior mean factor scores $\lambda_{i,i}^*$ as candidate predictors in a survival analysis of the breast cancer patient data.

We use Weibull regression models of patient survival that draw on the 30 estimated neutralization/lactic acidosis pathway factors, the 7 original projected signature scores, and the clinical covariates available for this data set (18). The latter include histologic grade, ER mutation status, node status, P53 mutation status, PgR mutation status, tumor size, and age at diagnosis. This analysis allows both integration and comparison of the prognostic value of these traditional markers with specific pathway-related signature scores, and their latent factor representations – an integrative clinico-genomic analysis (18; 25; 20; 1; 6; 19; 7; 22) Let t_i denote the survival time of patient i . The Weibull density function is $p(t_i|a, \gamma) = at_i^{a-1} \exp(\eta_i - t_i^a e^{\eta_i})$ where $a > 0$ is the index parameter and $\eta_i = \gamma' y_i$ the linear predictor based on a covariate vector y_i . We explore subsets of covariates and regression model uncertainty using Bayesian shotgun stochastic search (SSS: 10; 11). This generates a list of regression covariate subsets and the corresponding posterior regression model probabilities for use in Bayesian model averaging for survival prediction and in exploring relevance of variables. Details of model and prior specification follow defaults in the SSS software (11) as noted in the appendix below.

Figure 6 shows posterior probabilities for each of the 46 candidate covariates. Nodal status emerges as the leading predictor of long term survival, followed by latent factor 30 and then tumor size. Note that none of the original signature scores, and no other clinical variables, receive appreciable probability. That nodal status provides the best predictor of survival is to be expected. Previous studies (25; 20; 7) have shown that nodal status is not well predicted by gene expression and that combined use of nodal status with gene expression predictors can improve survival prognosis. Hence it seems that the information content of the nodal status predictor is unlikely to overlap with that of any factor score. This can also be clearly seen through the pairwise inclusion probabilities in Figure 7.

1
2
3
4
5
6
7
8
9
10
11
12
13
14
15
16
17
18
19
20
21
22
23
24
25
26
27
28
29
30
31
32
33
34
35
36
37
38
39
40
41

1
2
3
4
5
6
7
8
9
10
11
12
13
14
15
16
17
18
19
20
21
22
23
24
25
26
27
28
29
30
31
32
33
34
35
36
37
38
39
40
41

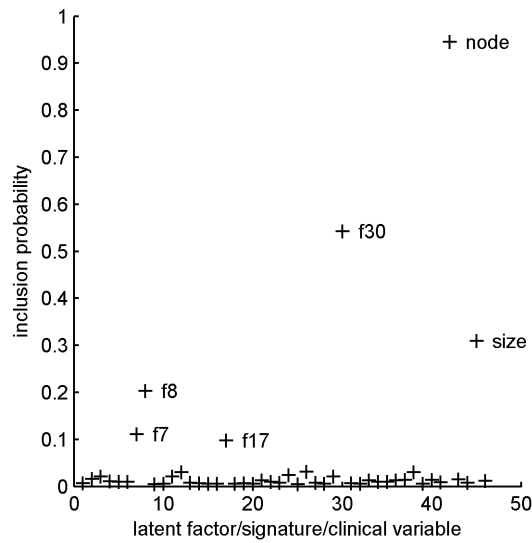


FIG 6. *Posterior inclusion probabilities for the 46 candidate covariates in the Weibull models. The candidate covariates include the 30 estimated latent factors, followed by the 7 original signature scores, followed by 10 traditional clinical covariates (Elston grades 1, 2, and 3, ER, node status, P53, PgR status, tumor size, age at diagnosis).*

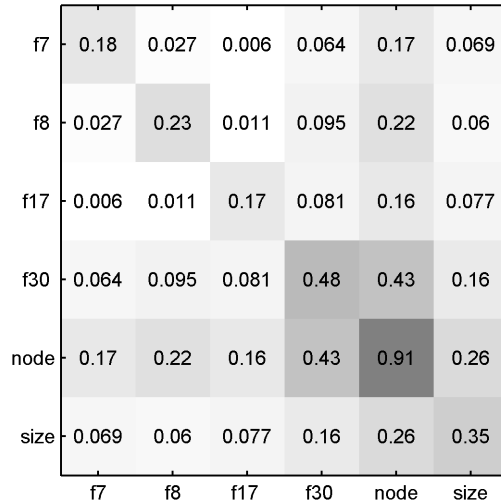


FIG 7. Pairwise inclusion probabilities for the top 6 predictor variables in breast cancer survival analysis. Darker colored tiles indicate higher probabilities.

The pairwise inclusion probability of factor 30 and nodal status is close to the marginal probability of factor 30; however, the pairwise inclusion probability of factor 30 with any of the other factors is far less than any of the marginal inclusions probabilities of those factors; thus factor 30 is clearly a dominant and preferred expression-based biomarker of survival risk.

Posterior and predictive inferences are formally based on a mixture of 1,000 Weibull survival models, mixed with respect to their posterior probabilities. For each patient i , we can compute the implied predicted survival function at her covariate vector y_i and identify the predicted median survival m_i ; this is the predicted median survival time for a *future* patient who has the same covariates as patient i . Figure 8(a) shows a Kaplan-Meier survival plot of the Miller *et al* data simply stratified by $m_i \leq m$ or $m_i > m$ where $m = \text{median}\{m_i, i = 1, \dots, n\}$. There is approximately a 30% difference in the empirical 10-year survival probability between patients cohorts stratified crudely on this basis, as a simple visual of the relevance of the included covariates. By way of focusing on factor 30, we plot the model-averaged survival curve for a hypothetical patient whose covariates are held constant at their median values in the data set, save for variation in the factor 30 score; see Figure 8(b), where factor 30 is set at its 5th, 50th, and 95th per-

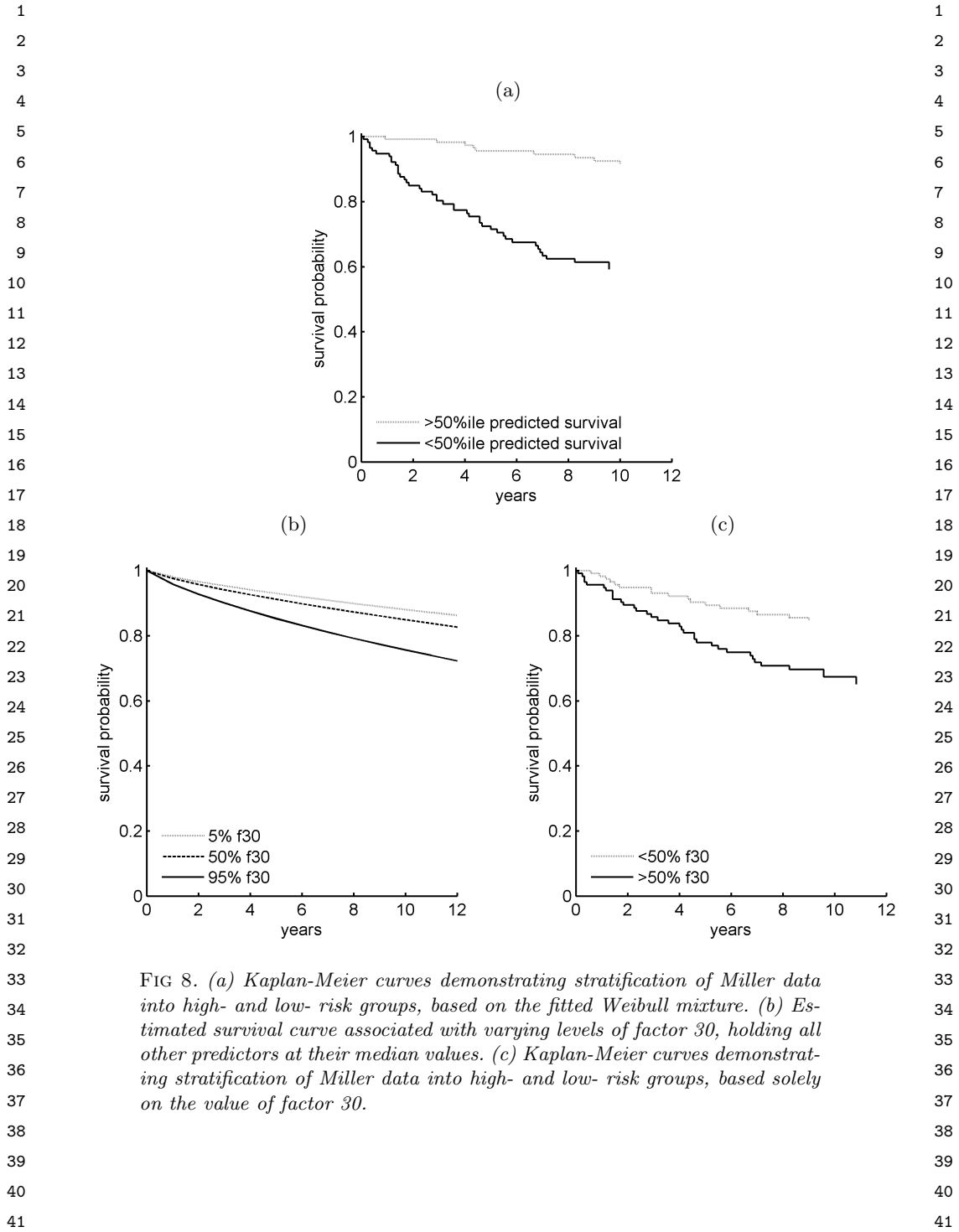


FIG 8. (a) Kaplan-Meier curves demonstrating stratification of Miller data into high- and low- risk groups, based on the fitted Weibull mixture. (b) Estimated survival curve associated with varying levels of factor 30, holding all other predictors at their median values. (c) Kaplan-Meier curves demonstrating stratification of Miller data into high- and low- risk groups, based solely on the value of factor 30.

centiles in the data set, all other covariates remaining fixed. The estimated effect of variation in factor 30 alone accounts for approximately 20% of the difference in 10-year patient survival between the high-risk and low-risk subgroups. This prediction is confirmed by considering the Kaplan-Meier curves formed by stratifying the patients on the basis of the patient-specific factor 30 value compared to the median across samples; see Figure 8(c). The pattern of gene expression comprising the loading associated with factor 30 warrants further investigation, to which we will return in Section 4.3.

4.2. Out-of-sample Factor Projection. It is critical to evaluate whether or not the above results can be confirmed through out-of-sample prediction. We do this with two additional breast cancer data sets: that of Pawitan *et al* (19), consisting of 159 primary breast tumors assayed on Affymetrix U133A and U133B chips, and that of Sotiriou *et al* (22), consisting of 189 primary breast tumors assayed on U133A chips.

Fixing all factor model parameters at their posterior means, we can directly predict values of the latent factors for each new patient; see appendix below and (16). Note that this calculation purely predictive; no model fitting nor additional analysis of the two validation data sets was performed. Using the predicted latent factor vectors, we can produce the same survival plots for these data, stratifying each of the two new patient cohorts on the basis of their factor 30 scores as above, see Figure 9, as compared to Figure 8(c). The association between low factor 30 scores and good prognosis remains evident in these out-of-sample predictions that draw on different patient populations. Further, the differences between high and low risk groups is comparable across all three samples.

The robustness of factor 30 as a prognostic biomarker provides strong support for the view that it reflects a biologically meaningful module of gene expression. By evaluating the predicted factor scores in the original experimental data, we are able to establish that factor 30, despite its relatively late incorporation to the model, is linked to the 4-hour lactic acidosis pathway. Figure 10 compares the predicted factor scores for factors 1 and 30 as evaluated in the experimental data. Factor 1, which is founded by the 4-hour lactic acidosis signature, is in fact comparable to the original signature score as depicted in Figure 2. Factor 30 has its highest values in the original 4-hour lactic acidosis samples, but shows a different pattern of activity across the other sample cohorts. In particular, factor 30 appears to be repressed in the samples associated with the 4-hour neutralization and acidic growth treatments. This implies that factor 30 may characterize some critical intersection between these pathways that is itself related to tumor

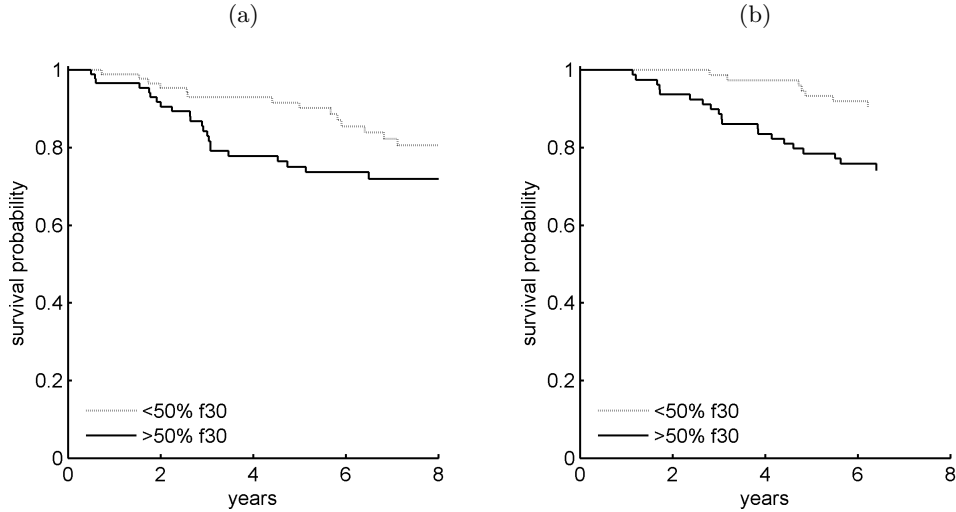


FIG 9. Kaplan-Meier curves demonstrating stratification of (a) the Pawitan et al (19) patient samples, and (b) the Sotiriou et al (22) patient samples (right) into high- and low- risk groups based on imputed values of factor 30, as identified in the latent factor analysis of the Miller data.

aggressiveness.

4.3. *Biological Evaluation of Prognostic Factor 30.* Having established the clinical relevance of factor 30, the task remains to ascribe to it biological meaning. The loading of factor 30 is comprised of only 6 gene probe sets for which $\pi_{g,l}^* > 0.99$. Four of these, including the founder gene, are related to the phosphoglycerate kinase 1 (PGK1) gene, while the other two are related to a neuronal cell death-related protein and the CEGP1 protein. The factor is characterized by overexpression ($\beta_{g,k} > 0$) of the PGK1 and neuronal cell death proteins and suppression ($\beta_{g,k} < 0$) of CEGP1.

A literature search generates detailed biological information on PGK1, and its role in the glycolysis pathway where it is fundamental to cell growth and metabolism. PGK1 catalyzes the reversible conversion of 1,3, diphosphoglycerate to 3-phosphoglycerate with the generation of one molecule of ATP and this represents an important step in glycolysis pathways. In addition, PGK1 has been reported to induce other processes related to cancer progression, such as conferring a multi-drug resistant (MDR) phenotype (8) and affecting tumor angiogenesis through affecting secreted plasmin (14). Previous studies have also shown that elevated levels of PGK1 predict *poor* survival outcomes in lung cancers (3), and that PGK1 can often be expressed

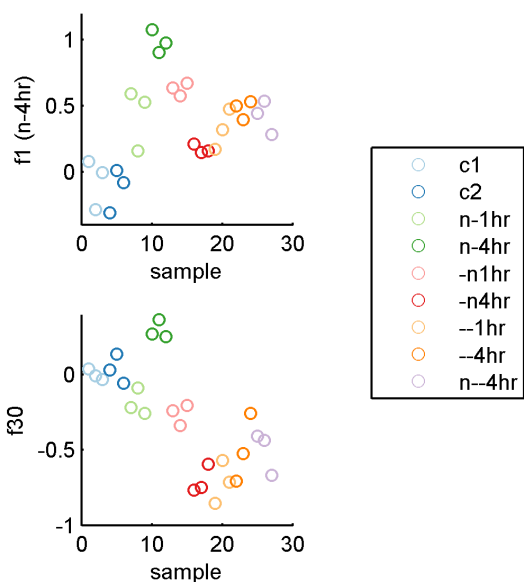


FIG 10. Predicted values of factors 1 and 30 for each sample in the original experimental study. Separate treatment groups are color coded.

at high levels in pancreatic (12) and renal (23) cancers. The association between high factor 30 levels and poor prognosis indicates a similar relationship between PGK1 and survival may exist for breast cancers.

Since PGK1 is an important component of glycolysis pathways, our findings here may implicate glycolysis activities in poor patient survival. This is supported by previous findings that expression of glycolysis pathways and PGK1 are repressed by lactic acidosis (4). Factor 30 links the neutralization pathway response signatures to a clear *PGK1* factor that may now serve as a biomarker of one key aspect of tumor responses to changes in pH with the potential to aid in predicting follow-on changes in tumor metabolism via glycolysis pathway activation. Further evaluation of this chain of relationships is now initiated and will be explored using independent methods such as tumor tissue microarrays (3). Since PGK1 and glycolysis pathways are also controlled by hypoxia (5), these results also highlight their potential roles as as integral mediators of multiple micro-environmental factors affecting tumor progression and clinical outcomes.

Acknowledgements. The authors are grateful to an editor of AOAS and an anonymous reviewer for constructive comments on this manuscript.

1 Research partially supported by National Science Foundation (DMS-0342172) 1
 2 and National Institutes of Health (NCI U54-CA-112952). Any opinions, find- 2
 3 ings and conclusions or recommendations expressed in this work are those 3
 4 of the authors and do not necessarily reflect the views of the NSF or NIH. 4
 5

6 **Supplementary Material: Code and data.** Further details and com- 6
 7 plete information needed to recapitulate the analyses reported are available 7
 8 at <http://ftp.stat.duke.edu/WorkingPapers/08-34.html> This includes 8
 9 all data files, files for model specification used as inputs to the BFRM and 9
 10 SSS Weibull regression software, and all corresponding text files of analysis 10
 11 summaries. The site also includes links to the freely available BFRM and 11
 12 SSS software for model implementation. 12
 13

14 Appendix. 14

15 *Prior specification for sparse regression model.* In the sparse regression 15
 16 model of the *in-vitro* data in Section 2.2, the prior specification is, following 16
 17 (15), 17
 18

$$\begin{aligned}
 \beta_{g,k} &\sim (1 - \pi_{g,k})\delta_0 + \pi_{g,k}N(0, \tau_k) & 19 \\
 \pi_{g,k} &\sim (1 - \rho_k)\delta_0 + \rho_k Be(9, 1) & 20 \\
 \rho_k &\sim Be(0.002, 19.998) & 21 \\
 \tau_k &\sim IG(5, 1) & 22
 \end{aligned}$$

23 with $\mu_g \sim N(8, 100)$, $\nu_{g,i} \sim N(0, \psi_g)$, and $\psi_g \sim IG(2, 0.005)$. Hyperpa- 23
 24 rameters for the distributions on μ_g and ψ_g are chosen to reflect ranges of 24
 25 expression variation and gene-specific uncertainty using Affymetrix microar- 25
 26 ray data. Hyperparameters for the sparsity-related parameters ($\pi_{g,k}$ and ρ_k) 26
 27 represent a weak prior belief that few genes will show a response to a partic- 27
 28 ular experimental intervention, with magnitudes of non-zero effects having 28
 29 treatment-specific variances (τ_k). 29
 30
 31
 32

33 *Prior specification for sparse factor model.* In the sparse factor model 33
 34 of the *in-vivo* data in Section 3.2, elements of A (regression coefficients and 34
 35 factor loadings) are modelled independently with hierarchical sparsity priors 35
 36 as in the regression model. Prior distributions are, for the most part, as de- 36
 37 scribed above. The baseline expression levels are again $\mu_g \sim N(8, 100)$, and 37
 38 idiosyncratic noise is modelled as $\nu_{g,i} \sim N(0, \psi_g)$ with $\psi_g \sim IG(2, 0.005)$. 38
 39
 40
 41

ran for 10,000 iterates and recorded details on the 1,000 highest posterior probability models (the null model is not among these 1,000); these models generate the posterior summaries discussed in Section 4.1.

Factor Projection to New Samples. Projecting inferences from factor model analyses in order to predict values of latent factors in new samples, used in the validation survival analysis in Section 4.2, follows theory and methods in (16). Based on all model parameters fixed at their posterior mean estimates (but here dropping the superscript * that denotes that, for notational clarity), the Dirichlet process prior on factor scores leads easily to computation of posterior predicted factor values on a new sample. Let A_L be the 500×30 dimensional portion of the estimated factor loadings matrix corresponding to latent factors only, and let Ψ_L be the diagonal matrix of estimated variance terms of the $\nu_{g,i}$ for this set of 500 scores and genes. Similarly, let λ_i be the estimated 30-vector of latent factors only on tumor sample i , ($i = 1, \dots, n = 251$). Then, for a 500-vector observation x on a new sample, the vector of imputed values of the 30 latent factor scores is

$$f = c_0 f + \sum_{i=1}^n c_i \lambda_i$$

where

$$f = (I_{30} + A_L' \Psi A_L)^{-1} A_L' \Psi_L x$$

with

$$c_0 \propto \alpha N(x|0, A_L A_L' + \Psi_L) \quad \text{and} \quad c_i \propto N(x|A_L \lambda_i, \Psi_L), \quad i > 0.$$

Note that α here is the estimated total mass parameter from the Dirichlet process component of the factor model (and output from the BFRM analysis), and the c_i are normalized to sum to one over $i = 0, 1, \dots, n$.

References.

- [1] BILD, A., YAO, G., CHANG, J., WANG, Q., POTTI, A., CHASSE, D., JOSHI, M., HARPOLE, D., LANCASTER, J., BERCHUCK, A., OLSON, J., MARKS, J., DRESSMAN, H., WEST, M., and NEVINS, J. (2006) Oncogenic pathway signatures in human cancers as a guide to targeted therapies. *Nature*. **439**:353-357.
- [2] CARVALHO, C., CHANG, G., LUCAS, J., NEVINS, J.R., WANG, Q., and WEST, M. (2008) High-dimensional sparse factor modelling: Applications in gene expression genomics. *Journal of the American Statistical Association*. **103**:1438-1456.
- [3] CHEN, G., GHARIB, T. G., WANG, H., HUANG, C. C., KUICK, R., THOMAS, D. G., SHEDDEN, K. A., MISEK, D. E., TAYLOR, J. M., GIORDANO, T. J. ET AL. (2003) Protein profiles associated with survival in lung adenocarcinoma. *Proc Natl Acad Sci USA* **100**:13537-13542.

- 1 [4] CHEN, J. L., LUCAS, J. E., SCHROEDER, T., MORI, S., NEVINS, J. R., DEWHIRST, 1
2 M. W., WEST, M., and CHI J. T. (2008) Genomic analysis of response to lactic 2
3 acidosis and acidosis in human cancers. *PLoS Genetics* **4**. 3
4 [5] CHI, J. T., WANG, Z., NUYTEN, D. S., RODRIGUEZ, E. H., SCHANER, M. E., SALIM, 4
5 A., WANG, Y., KRISTENSEN, G. B., HELLAND, A., BORRESEN-DALE, A. L. ET AL. 5
6 (2006) Gene expression programs in response to hypoxia: Cell type specificity and 6
7 prognostic significance in human cancers. *PLoS Medicine* **3**:e47. 7
8 [6] CHIN, K., DEVRIES, S., FRIDLAND, J., SPELLMAN, P., ROYDASGUPTA, R., KUO, 8
9 W-L., LAPUK, A., NEVE, R., QIAN, Z., RYDER, T., CHEN, F., FEILER, H., 9
10 TOKUYASU, T., KINGSLEY, C., DAIRKEE, S., MENG, Z., CHEW, K., PINKEL, D., 10
11 JAIN, A., LJUNG, B., ESSERMAN, L., ALBERTSON, D., WALDMAN, F., and GRAY, J. 11
12 (2006) Genomic and transcriptional aberrations linked to breast cancer pathophysiol- 12
13 ogy. *Cancer Cell*. **10**:529-541. 13
14 [7] DRESSMAN, H. K., HANS, C., BILD, A., OLSON, J., ROSEN, E., MARCOM, P., 14
15 LIOCHEVA, V., JONES, E., VUJASKOVIC, Z., MARKS, J., DEWHIRST, M., WEST, 15
16 M., NEVINS, J., and BLACKWELL, K. (2006) Gene expression profiles of multiple 16
17 breast cancer phenotypes and response to neoadjuvant chemotherapy. *Clin Cancer 17*
18 *Res.* **12**:819-826. 18
19 [8] DUAN, Z., LAMENDOLA, D. E., YUSUF, R. Z., PENSON, R. T., PREFFER, F. I., and 19
20 SEIDEN, M. V. (2002) Overexpression of human phosphoglycerate kinase 1 (PGK1) 20
21 induces a multidrug resistance phenotype. *Anticancer Research*. **22**:1933-1941. 21
22 [9] HANAHAN, D. and WEINBERG, R. (2000) The Hallmarks of Cancer. *Cell* **100**:57-70. 22
23 [10] HANS, C., DOBRA, A. and WEST, M. (2007) Shotgun stochastic search in regression 23
24 with many predictors. *Journal of the American Statistical Association*. **102**:507-516. 24
25 [11] HANS, C., WANG, Q., DOBRA, A. and WEST, M. (2007) SSS: High-dimensional 25
26 Bayesian regression model search. *Bulletin of the International Society for Bayesian 26*
27 *Analysis*. **14**:8-9. 27
28 [12] HWANG, T. L., LIANG, Y., CHIEN, K. Y., and YU, J. S. (2006) Overexpression and 28
29 elevated serum levels of phosphoglycerate kinase 1 in pancreatic ductal adenocarci- 29
30 noma. *Proteomics* **6**:2259-2272. 30
31 [13] IRIZARRY, R., BOLSTAD, B., COLLIN, F., COPE, L., HOBBS, B., and SPEED, T. 31
32 (2003) Summaries of Affymetrix GeneChip probe level data. *Nucleic Acids Research*. 32
33 **31**:e15. 33
34 [14] LAY, A. J., JIANG, X. M., KISKER, O., FLYNN, E., UNDERWOOD, A., CONDRON, 34
35 R., and HOGG, P. J. (2000) Phosphoglycerate kinase acts in tumour angiogenesis as 35
36 a disulphide reductase. *Nature* **408**:869-873. 36
37 [15] LUCAS, J., CARVALHO, C., WANG, Q., BILD, A., NEVINS, J., and WEST, M. (2006) 37
38 Sparse statistical modelling in gene expression genomics. In *Bayesian Inference for 38*
39 *Gene Expression in Proteomics*. Eds. Müller, P., Do, K. A., and Vannucci, M. Cam- 39
40 bridge University Press, 155-176. 40
41 [16] LUCAS, J., CARVALHO, C., MERL, D., and WEST, M. (2008) In-vitro to In-vivo 41
42 factor profiling in expression genomics. *Bayesian Modeling in Bioinformatics*. Eds 42
43 Dey, D., Ghosh, S., and Mallick, B. Taylor Francis, **in press**. 43
44 [17] LUCAS, J., CARVALHO, C., and WEST, M. (2009) A Bayesian Analysis Strategy for 44
45 Cross-Study Translation of Gene Expression Biomarkers. *Statistical Applications in 45*
46 *Genetics and Molecular Biology* **8**:art11. 46
47 [18] MILLER, L.D., SMEDS, J., GEORGE, J., VEGA, V.B., VERGARA, L., PLONER, A., 47
48 PAWITAN, Y., HALL, P., KLAAR, S., LIU, E. T., and BERGH, J. (2005) An expression 48
49 signature for p53 status in human breast cancer predicts mutation status, transcrip- 49
50 tional effects, and patient survival. *Proceedings of the National Academy of Sciences*. 50
51 51

- 1 **102**:13550-13555. 1
- 2 [19] PAWITAN, Y., BJOHLE, J., AMLER, L., BORG, A., EGYHAZI, S., HALL, P., HAN, 2
- 3 X., HOLMBERG, L., HUANG, F., SLAAR, S., LIU, E., MILLER, M., NORDGREN, H., 3
- 4 PLONER, A., SANDELIN, K., SHAW, P., SMEDS, J., SKOOG, L., WEDREN, S., and 4
- 5 BERGH, J. (2005) Gene expression profiling spares early breast cancer patients from 5
- 6 adjuvant therapy: Derived and validated in two population-based cohorts. *Breast 6*
- 7 *Cancer Research*. **7**:R953-R964 7
- 8 [20] PITTMAN, J., HUANG, E., DRESSMAN, H., HORNG, C. F., CHENG, S. H., TSOU, M. 8
- 9 H., CHEN, C. M., BILD, A., IVERSEN, E. S., HUANG, A. T., NEVINS, J. R., and 9
- 10 WEST, M. (2004) Integrated modeling of clinical and gene expression information for 10
- 11 personalized prediction of disease outcomes. *Proceedings of the National Academy of 11*
- 12 *Sciences*. **101**:8431-8436. 12
- 13 [21] SEO, D.M., GOLDSCHMIDT-CLERMONT, P.J. and West, M. (2007) Of mice and men: 13
- 14 Sparse statistical modelling in cardiovascular genomics. *Annals of Applied Statistics*, 14
- 15 **1**:152-178. 15
- 16 [22] SOTIRIOU, C., WIRAPATI, P., LOI, S., HARRIS, A., FOX, S., SMEDS, J., NORDGREN, 16
- 17 H., FARMER, P., PRAZ, V., HAIBE-KAINS, B., DESMEDT, C., LARSIMONT, D., CAR- 17
- 18 DOSO, F., PETERSE, H., NUYTEN, D., BUYSE, M., VAN DE VIJVER, M., BERGH, J., 18
- 19 PICCART, M., and DELORENZI, M. (2006) Gene expression profiling in breast cancer: 19
- 20 Understanding the molecular basis of histologic grade to improve prognosis. *Journal 20*
- 21 *of the National Cancer Institute*. **98**: 262-272 21
- 22 [23] UNWIN, R. D., CRAVEN, R. A., HARNDEN, P., HANRAHAN, S., TOTTY, N., 22
- 23 KNOWLES, M., EARDLEY, I., SELBY, P. J., and BANKS, R. E. (2003) Proteomic 23
- 24 changes in renal cancer and co-ordinate demonstration of both the glycolytic and 24
- 25 mitochondrial aspects of the Warburg effect. *Proteomics* **3**:1620-1632. 25
- 26 [24] WANG, Q., CARVALHO, C., LUCAS, J., and WEST, M. (2007) BFRM: Bayesian factor 26
- 27 regression modelling. *Bulletin of the International Society for Bayesian Analysis*. 27
- 28 **14**:4-5. 28
- 29 [25] WEST, M., BLANCHETTE, C., DRESSMAN, H., HUANG, E., ISHIDA, S., SPANG, R., 29
- 30 ZUZAN, H., OLSON, J., MARKS, J., and NEVINS, J. (2001) Predicting the clinical 30
- 31 status of human breast cancer by using gene expression profiles. *Proceedings of the 31*
- 32 *National Academy of Sciences*. **98**:11462-11467. 32
- 33 [26] WEST, M. (2001) Bayesian factor regression models in the “large p, small n” 33
- 34 paradigm. *Bayesian Statistics 7*. Eds. Bernardo, J.M., Bayarri, M.J., Berger, J.O., 34
- 35 Dawid, A.P., Heckerman, D., Smith, A.F.M., and West, M. Oxford University Press, 35
- 36 723-732. 36
- 37 37
- 38 38
- 39 39
- 40 40
- 41 41

DANIEL MERL AND MIKE WEST
 DEPARTMENT OF STATISTICAL SCIENCE
 DUKE UNIVERSITY
 DURHAM NC 27708-0251
 E-MAIL: dan@stat.duke.edu
mw@stat.duke.edu

JULIA LING-YU CHEN AND JEN-TSAN CHI
 DUKE UNIVERSITY MEDICAL CENTER
 BOX 3382
 DURHAM NC 27710-3382
 E-MAIL: julia.chen@duke.edu
jentsan.chi@duke.edu